Transient activation of fission yeast AMPK is required for cell proliferation during osmotic stress

Katherine L. Schutt and James B. Moseley*
Department of Biochemistry and Cell Biology, Geisel School of Medicine at Dartmouth, Hanover, NH 03755

ABSTRACT **The heterotrimeric kinase AMPK acts as an energy sensor to coordinate cell metabolism with environmental status in species from yeast through humans. Low intracellular ATP leads to AMPK activation through phosphorylation of the activation loop within the catalytic subunit. Other environmental stresses also activate AMPK, but it is unclear whether cellular energy status affects AMPK activation under these conditions. Fission yeast AMPK catalytic subunit Ssp2 is phosphorylated at Thr-189 by the upstream kinase Ssp1 in low-glucose conditions, similar to other systems. Here we find that hyperosmotic stress induces strong phosphorylation of Ssp2-T189 by Ssp1. Ssp2-pT189 during osmotic stress is transient and leads to transient regulation of AMPK targets, unlike sustained activation by low glucose. Cells lacking this activation mechanism fail to proliferate after hyperosmotic stress. Activation during osmotic stress requires energy sensing by AMPK heterotrimer, and osmotic stress leads to decreased intracellular ATP levels. We observed mitochondrial fission during osmotic stress, but blocking fission did not affect AMPK activation. Stress-activated kinases Sty1 and Pmk1 did not promote AMPK activation but contributed to subsequent inactivation. Our results show that osmotic stress induces transient energy stress, and AMPK activation allows cells to manage this energy stress for proliferation in new osmotic states.**

Monitoring Editor
Daniel J. Lew
Duke University

Received: Apr 12, 2017
Revised: May 5, 2017
Accepted: May 9, 2017

INTRODUCTION

Cells require dynamic mechanisms to couple their metabolism to changes in the environment, but how different stress conditions signal to core metabolic regulators is not well understood. In eukaryotic cells, the serine/threonine AMP-activated protein kinase (AMPK) acts as a major sensor and regulator of intracellular energy. AMPK is a heterotrimeric protein kinase complex composed of α, β, and γ subunits. The catalytic α subunit contains the kinase domain; the γ subunit contains CBS domains that bind to adenosine nucleotides; and the β subunit is a scaffold that connects the α and γ subunits (Schmidt and McCartney, 2000; Scott *et al.*, 2004; Iseli *et al.*, 2005; Elbing *et al.*, 2006). Competitive binding of ATP versus ADP/AMP by the γ subunit controls allosteric rearrangements within the complex. When cellular ATP levels are high, the γ subunit binds to ATP, resulting in an inactive state for the heterotrimer. On a drop in cellular ATP levels, the γ subunit binds to AMP, and changes in the heterotrimer structure facilitate phosphorylation of the catalytic α subunit within its activation loop (Davies *et al.*, 1995; Jiang and Carlson, 1996; Wilson *et al.*, 1996; Rubenstein *et al.*, 2008). Specifically, this structural rearrangement is believed to inhibit the dephosphorylation rate of the activation loop by inhibitory phosphatases, thereby leading to higher levels of the phosphorylated, activated complex (Davies *et al.*, 1995; Jiang and Carlson, 1996; Suter *et al.*, 2006, Sanders *et al.*, 2007, Rubenstein *et al.*, 2008, Mayer *et al.*, 2011). Through this mechanism, AMPK senses the energy status of a cell based on the ratio of ATP versus AMP/ADP. Activated AMPK complex then switches cells to a catabolic state to promote cell survival. Several upstream kinases have been shown to phosphorylate human AMPK, most notably the tumor suppressor LKB1 (Hawley *et al.*, 2003; Woods *et al.*, 2003; Lizcano *et al.*, 2004). The critical role of AMPK in maintaining cellular metabolism has made it a prominent therapeutic target for cancer and other diseases such as type II diabetes (Shackelford and Shaw, 2009).

This article was published online ahead of print in MBoC in Press (http://www.molbiolcell.org/cgi/doi/10.1091/mbc.E17-04-0235) on May 17, 2017.

*Address correspondence to: James B. Moseley (james.b.moseley@dartmouth.edu).

Abbreviations used: AMPK, AMP-activated protein kinase; DHAP, dihydroxyacetone phosphate; G3P, glycerol-3-phosphate; SAPK, stress-activated protein kinase.

Beyond its canonical role in response to cellular energy changes, AMPK has been studied for its role in adaptation to a variety of other stresses, including heat stress (Corton *et al.,* 1994), hypoxia (Emerling *et al.,* 2009, Evans *et al.,* 2005), and osmotic stress (Barnes *et al.,* 2002; Fryer *et al.,* 2002; Hawley *et al.,* 2010; Jiang *et al.,* 2015; Luo *et al.,* 2015). For osmotic stress, it has been unclear whether AMPK activation follows the canonical mechanism or a distinct pathway. Some studies proposed that osmotic stress activates AMPK independently of a change in nucleotide levels (Fryer *et al.,* 2002; Emerling *et al.,* 2009; Luo *et al.,* 2015), suggesting a noncanonical activation mechanism. Alternatively, it has been reported that osmotic stress might cause an increase in the cellular AMP/ATP ratio, leading to AMPK activation through the canonical activation pathway (Davies *et al.,* 1995; Suter *et al.,* 2006; Sanders *et al.,* 2007; Hawley *et al.,* 2010). Differentiating between these models in human cells can be complicated because different cell types might invoke different mechanisms. Humans also express multiple isoforms of each AMPK subunit, adding to this complexity. Finally, human AMPK can be activated by multiple upstream kinases that act redundantly but are regulated differently. Distinguishing between these models is important for understanding why cells activate AMPK during osmotic stress.

Yeast cells present a complementary model to study AMPK activation under different environmental stresses. Similar to mammalian cells, budding yeast AMPK can be activated in response to low glucose, sodium ion stress, alkaline pH, and oxidative stress (Celenza and Carlson, 1986; Hong and Carlson, 2007). These cells require the catalytic AMPK α subunit to remain viable under these conditions, particularly sodium ion stress by NaCl (Hong and Carlson, 2007; Ye *et al.,* 2008), but it is unknown whether energy sensing by the heterotrimer is involved. Further, as in humans, budding yeast express multiple redundant activating kinases (Hong *et al.,* 2003; Nath *et al.,* 2003; Sutherland *et al.,* 2003). As an alternative to budding yeast, the fission yeast *Schizosaccharomyces pombe* represents a simplified organism to study regulation of AMPK. Unlike the complicated upstream regulatory network of human cells or even budding yeast, fission yeast cells express a single activating kinase (Ssp1), which phosphorylates the fission yeast AMPK α subunit (Ssp2) in glucose depletion (Hanyu *et al.,* 2009; Valbuena and Moreno, 2012; Deng *et al.,* 2017) or in nitrogen stress (Davie *et al.,* 2015). Of interest, nitrogen limitation has been proposed to activate fission yeast AMPK independently of cellular ATP and energy sensing by the heterotrimer (Davie *et al.,* 2015). These observations suggest that the canonical activation mechanism might be restricted to depletion of environmental energy sources such as glucose, with alternative mechanisms operating under different environmental stresses.

In this study, we screened environmental conditions and found that osmotic stress activated fission yeast AMPK as potently as glucose deprivation. AMPK activation by osmotic stress was transient, required for cell proliferation, and dependent on the intact heterotrimer. In addition, we found that cellular ATP levels decreased in response to osmotic stress, strongly suggesting that the underlying mechanism and downstream function follow canonical energy-sensing models.

RESULTS

AMPK (Ssp2) is transiently activated in response to osmotic stress

To identify conditions that activate AMPK in fission yeast, we exposed cells to a range of environmental stresses and then monitored the activating phosphorylation Ssp2-pT189 with a phosphospecific antibody. 1 M KCl, which generates both salt and osmotic stress, led to strong activation of Ssp2 (Figure 1A). Ssp2-pT189 was also induced by sorbitol (Figure 1A), which generates an osmotic stress but not a salt stress, indicating that osmotic stress leads to AMPK activation in fission yeast. This response differs from budding yeast AMPK, which was activated by salt stress but not by osmotic stress (Hong and Carlson, 2007). During hyperosmotic stress, the level of AMPK activation was similar to the strong activation by low-energy conditions (Figure 1A). Further, combining hyperosmotic stress with low glucose did not increase Ssp2-pT189 phosphorylation as compared with either stress alone (Figure 1A).

We tested the dynamics of Ssp2-pT189 during hyperosmotic stress. Unlike the cellular response to medium containing low glucose, which induces sustained activation of AMPK (Deng *et al.,* 2017), Ssp2-pT189 under hyperosmotic stress was transient. We observed a strong response at 5 min, followed by a decrease by 30 min and a return to basal levels by 60 min (Figure 1B). We confirmed this dynamic activation of AMPK results from osmotic stress by monitoring Ssp2-pT189 during sorbitol treatment or NaCl treatment and again observed an initial strong response followed by a decrease at later time points (Figure 1, C and D). These results contrast with the situation in budding yeast, in which AMPK phosphorylation was induced by salt stress but not by sorbitol, and phosphorylation was sustained (Hong and Carlson, 2007; Ye *et al.,* 2008).

To determine whether these Ssp2-pT189 dynamics indeed reflect transient activation of AMPK, we monitored localization of the transcription factor Scr1, which is a downstream target of active Ssp2 and the *S. pombe* orthologue of budding yeast Mig1 (DeVit *et al.,* 1997; Treitel *et al.,* 1998; Matsuzawa *et al.,* 2012). Scr1 localizes to the nucleus and negatively regulates the expression of a glucose transporter, Ght5, under high-glucose conditions (Saitoh *et al.,* 2015). Activation of Ssp2 leads to phosphorylation of Scr1 and its export from the nucleus, relieving transcriptional repression of Ght5 (Matsuzawa *et al.,* 2012, Saitoh *et al.,* 2015). We grew cells in a microfluidic chamber that enabled control of media with simultaneous imaging of cells. On shift to 1 M KCl, Scr1-GFP was exported out of the nucleus (Figure 1E). Some cells began to recover nuclear Scr1-GFP signal 30 min after the shift, and by 60 min, Scr1-GFP had returned to the nucleus (Figure 1F). These kinetics mirrored the dynamics of Ssp2-pT189 regulation. To control for effects from switching the input lines of the microfluidic device, we also performed experiments switching from one input line containing medium lacking KCl to a different input line containing the same medium. No changes in Scr1-GFP localization were observed in these "control" medium switches (Figure 1, E and F). We conclude that osmotic stress induces transient phosphorylation and activation of fission yeast AMPK, leading to transient regulation of downstream targets.

We next tested whether the degree of osmotic stress controls the level of AMPK activation. Indeed, the level of Ssp2-pT189 correlated with the concentration of KCl (Figure 2A), such that a low degree of osmotic stress led to low levels of AMPK activation. In all cases, AMPK activation was transient and completed by 60 min (Figure 2, B and C). Thus salt stress induces a dose-dependent response in AMPK activation through phosphorylation of Ssp2-T189.

Ssp1 is the upstream activating kinase under osmotic stress

Only one upstream activating kinase has been identified for fission yeast AMPK, in contrast to the multiple activating kinases observed in other organisms, such as human and budding yeast cells (Hong *et al.,* 2003; Nath *et al.,* 2003; Sutherland *et al.,* 2003; Hanyu *et al.,* 2009; Valbuena and Moreno, 2012; Davie *et al.,* 2015; Deng *et al.,* 2017).

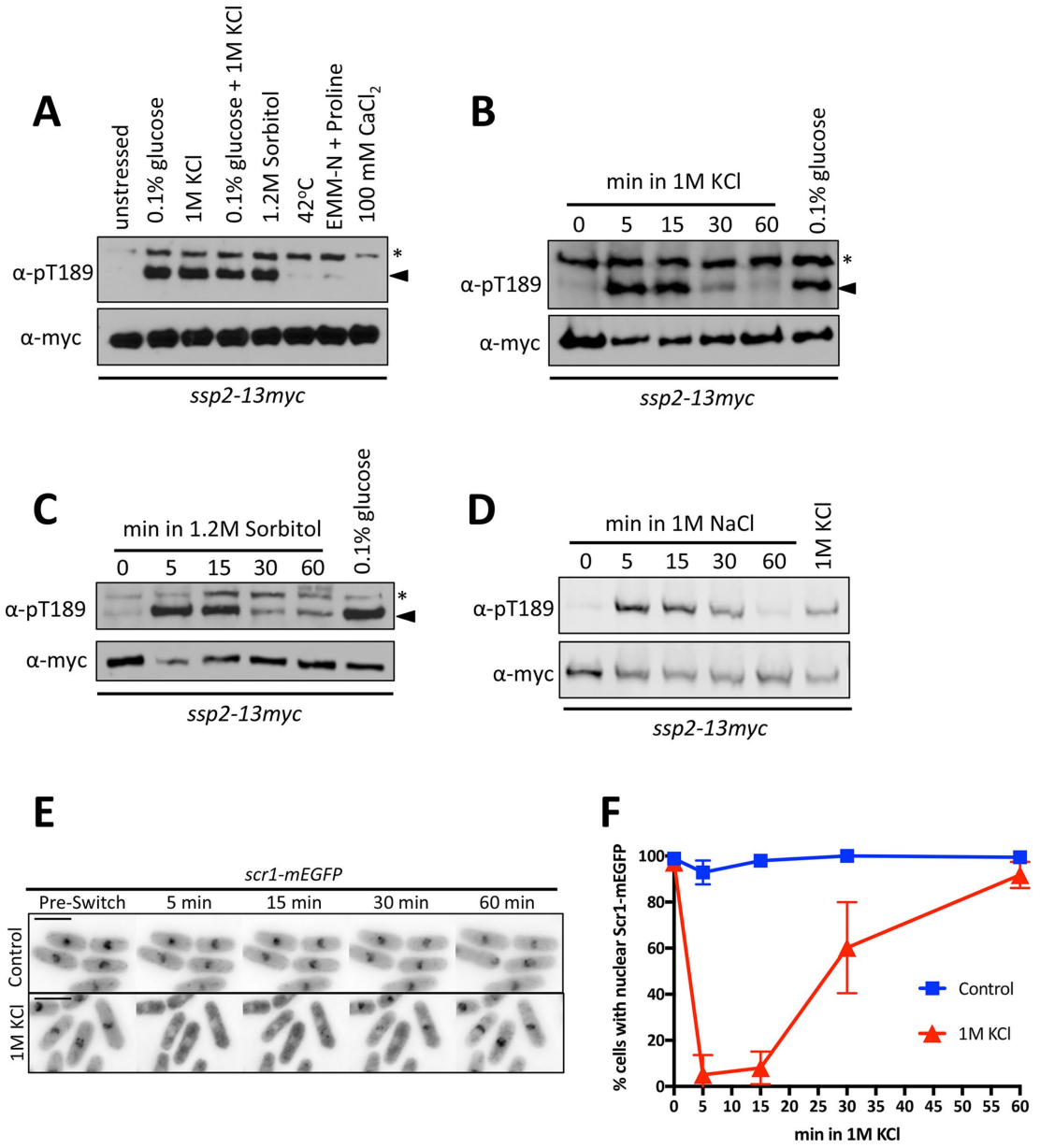

FIGURE 1: Transient activation of Ssp2 by hyperosmotic stress. (A) Western blot showing levels of Ssp2-pT189 in response to the indicated environmental stresses. Treatments were for 15 min. We used α-myc as a loading control for total Ssp2. For α-Ssp2-pT189, asterisks denote background bands, and arrowheads mark the Ssp2-pT189 band. (B) Western blot showing activation kinetics of Ssp2-pT189 in response to 1 M KCl. We used 0.1% glucose treatment as a control for Ssp2-pT189 induction and α-myc as a loading control for total Ssp2. (C) Western blot showing activation kinetics of Ssp2-pT189 in response to 1.2 M sorbitol. We used 0.1% glucose treatment as a control for Ssp2-pT189 induction and α-myc as a loading control for total Ssp2. (D) Western blot showing activation kinetics of Ssp2-pT189 in response to 1 M NaCl. We used 1 M KCl treatment as a control for Ssp2-pT189 induction and α-myc as a loading control for total Ssp2. (E) Localization of Scr1-mEGFP with control EMM4S treatment or EMM4S plus 1 M KCl treatment using a microfluidics device. Images are single focal planes. Preswitch indicates image taken before switch to control or 1 M KCl medium. Scale bar, 8 μm. (F) Quantification of Scr1-mEGFP nuclear localization from microfluidics-based movies as in E. More than 50 cells/condition. Mean ± SD based on three individual biological replicates.

We tested whether Ssp1, the kinase that phosphorylates Ssp2-T189 under low-energy and nitrogen stress, was responsible for AMPK activation during osmotic stress. Ssp2-pT189 was not detected in *ssp1*Δ mutant cells exposed to osmotic stress by 1 M KCl (Figure 3A). We conclude that Ssp1 is the upstream kinase for AMPK activation during osmotic stress and low glucose conditions, although the dynamics of activation are different for these two conditions.

We considered that the dynamics of Ssp2-T189 phosphorylation and dephosphorylation might reflect changes in Ssp1 activity. We tested this possibility by comparing Ssp2-pT189 dynamics with those of a different substrate of Ssp1. Previous work showed that Ssp1 phosphorylates the cell cycle kinase Cdr2 at residue T166 (Deng *et al.*, 2014). If Ssp2-T189 phosphorylation dynamics are caused by activation and inactivation of Ssp1 during osmotic

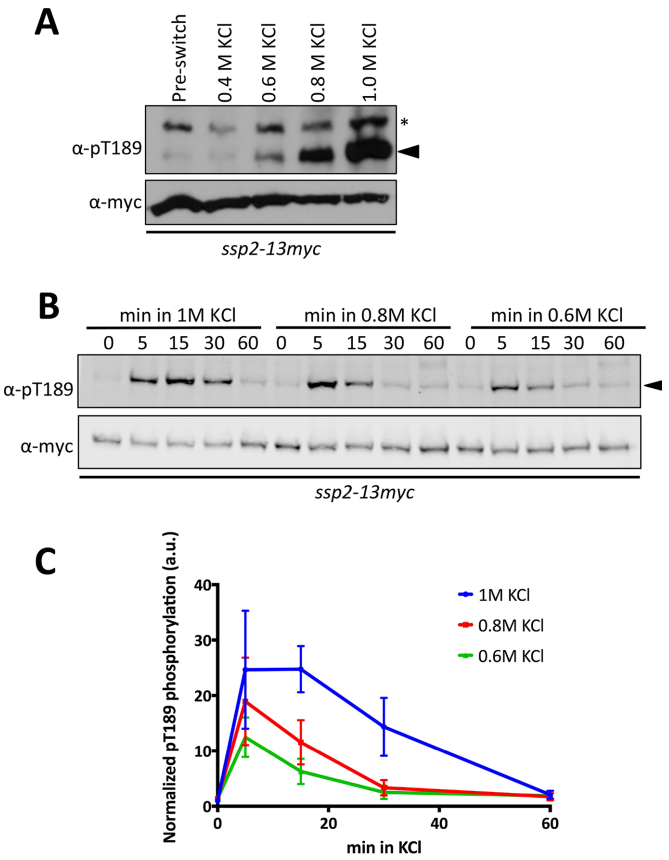

FIGURE 2: Osmotic stress activation of Ssp2 is dose dependent. (A) Western blot showing activation of Ssp2-pT189 in response to the indicated concentrations of KCl for 15 min. We used α-myc as a loading control for total Ssp2. For α-Ssp2-pT189, asterisks denote background bands, and arrowheads mark Ssp2-pT189 bands. (B) Western blot showing activation kinetics of Ssp2-pT189 in response to 1, 0.8, and 0.6 M KCl osmotic stress. We used α-myc as a loading control for total Ssp2. (C) Quantification of Ssp2-pT189 dynamics for the indicated concentrations of KCl. Mean ± SD based on three individual biological replicates.

stress, then similar dynamics should be observed for Cdr2-T166. In contrast to this prediction, we found that Cdr2-pT166 phosphorylation was unaffected by osmotic stress (Figure 3, B and C). Thus Ssp1 activates AMPK during osmotic stress, but changes in Ssp1 kinase activity are unlikely to explain the dynamics of this response.

To investigate the functional importance of Ssp1-AMPK signaling during osmotic stress, we monitored cell growth in mutant strains (Figure 3D). We observed strong growth defects for *ssp1*Δ cells on plates containing 0.8 M KCl, consistent with previous results (Rupeš *et al.*, 1999; Freitag *et al.*, 2014). Of interest, we observed identical growth defects for *ssp2*Δ and *ssp2(T189A)*, which contains a single point mutation that prevents phosphorylation of AMPK by Ssp1. These results show that Ssp1-AMPK signaling functions to maintain cell growth and survival during osmotic stress. We also tested whether Cdr2 contributes to cell growth during osmotic stress, but neither *cdr2*Δ nor *cdr2(T166A)* mutants exhibited growth defects, and these mutations did not exacerbate the defects of *ssp2* mutants. We conclude that AMPK is a critical target of Ssp1 for cell growth during osmotic stress.

As a final test for Ssp2 function in cell proliferation under osmotic stress, we used microfluidics to image wild type and *ssp2*Δ mutants during this stress. Wild-type and *ssp2*Δ mutant cells were mixed and loaded together in the same microfluidics chamber for simultaneous imaging under identical conditions. The wild-type cells (but not the *ssp2*Δ cells) expressed a mitochondrial matrix targeted–fluorescent mCherry (*mtmCherry*) protein so that we could distinguish the two strains in the same imaging field. On switch to medium containing 1 M KCl, both strains exhibited mechanical shrinkage typical of hyperosmotic stress. However, only wild-type cells adapted and resumed proliferation after this initial response (Figure 4A). After shift to medium with 1 M KCl, the number of wild-type cells increased from 10 to 44, and the number of *ssp2*Δ mutant cells increased from 7 to 8 (Figure 4B). Thus AMPK is required for cells to resume growth and proliferation when exposed to osmotic stress.

AMPK heterotrimer is essential for Ssp2 activation and cell survival under osmotic stress

The canonical role of the AMPK heterotrimer as a sensor of cellular energy status requires the nucleotide-binding γ subunit, which is physically connected to the catalytic α subunit by the scaffolding β subunit (Iseli *et al.*, 2005). Consistent with this model, in fission yeast, the intact heterotrimer is essential for adaptation to low-glucose medium (Matsuzawa *et al.*, 2012; Saitoh *et al.*, 2015; Deng *et al.*, 2017). A different mechanism has been proposed for nitrogen stress, in which Ssp1 activates Ssp2 in a heterotrimer-independent manner (Davie *et al.*, 2015). This heterotrimer-independent activation regulated mitotic entry during nitrogen stress and revealed a form of Ssp2 activation independent of the ATP/AMP ratio (Davie *et al.*, 2015). We sought to determine whether the intact heterotrimer was required for Ssp2 activation under osmotic stress by monitoring Ssp2-pT189 in *cbs2*Δ and *amk2*Δ mutants (γ- and β-subunit deletions, respectively). We did not detect Ssp2-pT189 in these mutants during osmotic stress or low glucose (Figure 5A). This result indicates that the intact heterotrimer is essential for activation under osmotic stress. The requirement for both regulatory subunits, Cbs2 and Amk2, for Ssp2 phosphorylation supports a mechanism in which canonical, heterotrimer-dependent sensing of cellular energy status is involved in Ssp2 activation during both osmotic stress and low-glucose conditions.

Phosphorylation of Ssp2-T189 during osmotic stress required the intact AMPK heterotrimer, and this activation step was required for cell growth during osmotic stress. These combined results predict that the intact AMPK heterotrimer should be required for cell growth during osmotic stress. We used serial dilution growth assays to monitor *cbs2*Δ and *amk2*Δ mutants during osmotic stress and found that these mutants exhibited growth defects in the presence of 0.8 M KCl, similar to *ssp2*Δ (Figure 5B). These data indicate that both Ssp2 activity and the intact heterotrimer are essential for cell proliferation under hyperosmotic stress.

The requirement for the AMPK regulatory subunits Cbs2 and Amk2 raised the possibility that osmotic stress decreases the energy status of cells, resulting in activation of Ssp2 through canonical energy-sensing mechanisms. To test this possibility, we measured intracellular ATP levels after 5-min exposure to osmotic stress, or low glucose, or in unstressed conditions (Figure 5C). Depletion of glucose from the medium led to a strong loss of cellular ATP levels, as expected. Of interest, we also detected a strong and significant reduction in cellular ATP levels during osmotic stress. We conclude that osmotic stress depletes cellular ATP levels, leading to AMPK activation through canonical energy sensing by the intact heterotrimer. This activation is required for cells to resume growth in their new osmotic environment.

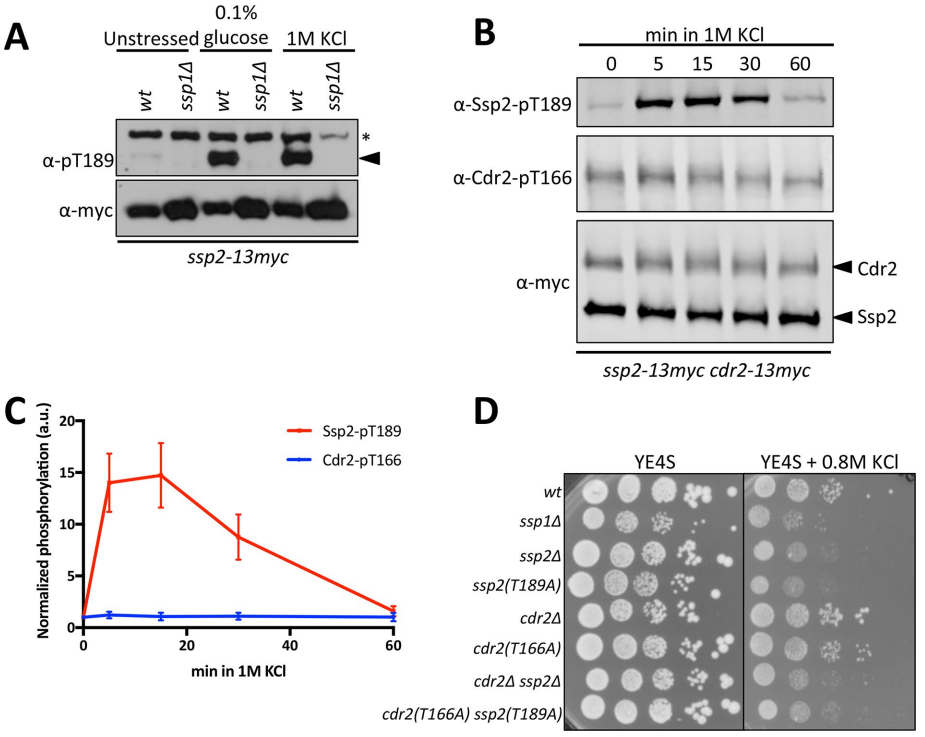

FIGURE 3: Ssp1 activates Ssp2 for cell proliferation in osmotic stress. (A) Western blot showing activation of Ssp2-pT189 in wild-type and *ssp1*Δ cells in response to 15 min of the indicated treatments. We used α-myc as a loading control for total Ssp2. For α-Ssp2-pT189, asterisks denote background bands, and arrowheads mark Ssp2-pT189 bands. (B) Western blot showing activation kinetics of Ssp1 substrates Ssp2-pT189 and Cdr2-pT166 in response to 1 M KCl osmotic stress. We used α-myc as a loading control for both Ssp2 and Cdr2. (C) Quantification of Ssp2-pT189 and Cdr2-pT166 levels in response to 1 M KCl. Mean ± SD based on three individual biological replicates. (D) Tenfold serial dilutions of the indicated strains were spotted onto control (YE4S) plates or plates containing 0.8 M KCl. Cells were grown at 32°C.

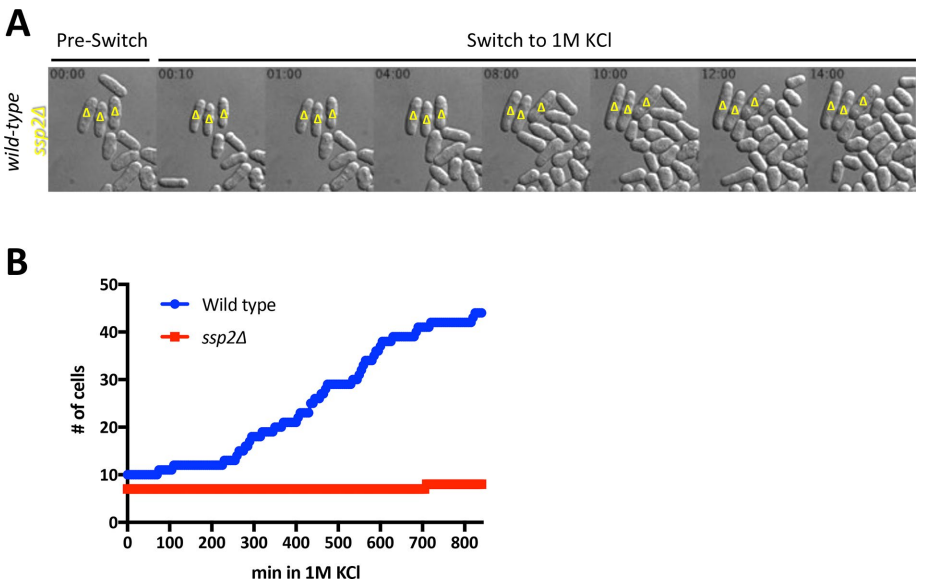

FIGURE 4: *ssp2*Δ mutants arrest growth and division during osmotic stress. (A) Differential interference contrast (DIC) images of selected time points for wild-type or *ssp2*Δ cells growing in a microfluidics device before and after exposure to 1 M KCl. Yellow triangles indicate *ssp2*Δ cells; unmarked cells are wild type. Time is indicated in hours:minutes. (B) Quantification of total cell number for wild-type vs. *ssp2*Δ strains after shift to 1 M KCl. Cells were imaged in time lapse using microfluidics, as in A. Cells were manually counted from each time frame, and only cells that were present in the imaging field throughout the entire experiment were counted.

Mitochondrial morphology during osmotic stress

We examined the possibility that ATP levels decrease during osmotic stress because of changes to mitochondria, the primary source of ATP generation. To monitor mitochondrial morphology during osmotic stress, we imaged cells expressing a mitochondrial matrix-targeted mCherry (*mtmCherry*). Before switch to hyperosmotic conditions, mitochondria appeared as elongated tubules characteristic for fission yeast cells. However, upon osmotic stress, these tubules lost their elongated appearance and resembled beads on a string (Figure 6, A and B). Recent work has shown that activated AMPK can induce mitochondrial fission in mammalian cells (Toyama *et al.*, 2016), suggesting the mitochondrial fragmentation that we observed could be a consequence of AMPK activation rather than a cause. However, mitochondria still fragmented in *ssp2*Δ mutant cells during osmotic stress (Figure 6, B and C). Thus AMPK activation during osmotic stress is not required for mitochondrial fragmentation. Note that mitochondrial morphology is affected in *ssp2*Δ cells, demonstrated by higher levels of unstressed cells expressing beads-on-a-string morphology. However, there is still a significant increase in the number of cells with affected morphology upon exposure to 1 M KCl (Figure 6, B and C).

We considered the possibility that mitochondrial fragmentation during osmotic stress might contribute to AMPK activation. To test this idea, we blocked mitochondrial fission by using *dnm1*Δ *vps1*Δ mutant cells, which lack the GTPases essential for fission (Jourdain *et al.*, 2008). The elongated mitochondria in these cells did not fragment upon osmotic stress (Figure 6, B–D), meaning that fragmentation likely reflects active fission by the physiological machinery. Despite the loss of mitochondrial fission and fragmentation, dynamic activation of AMPK was still observed in *dnm1*Δ *vps1*Δ cells during osmotic stress. The kinetics of Ssp2-T189 phosphorylation and dephosphorylation were similar to that of wild-type cells (Figure 6E). Further, we detected no growth defects for *dnm1*Δ, *vps1*Δ, or *dnm1*Δ *vps1*Δ cells on plates containing 0.8 M KCl (Figure 6F). We conclude that mitochondria undergo fission during osmotic stress, but this process is not responsible for AMPK activation and is not required for cell growth under these conditions.

Stress-activated protein kinase pathways contribute to Ssp2 inactivation under osmotic stress

Yeast cells activate multiple stress-activated protein kinase (SAPK) pathways in response

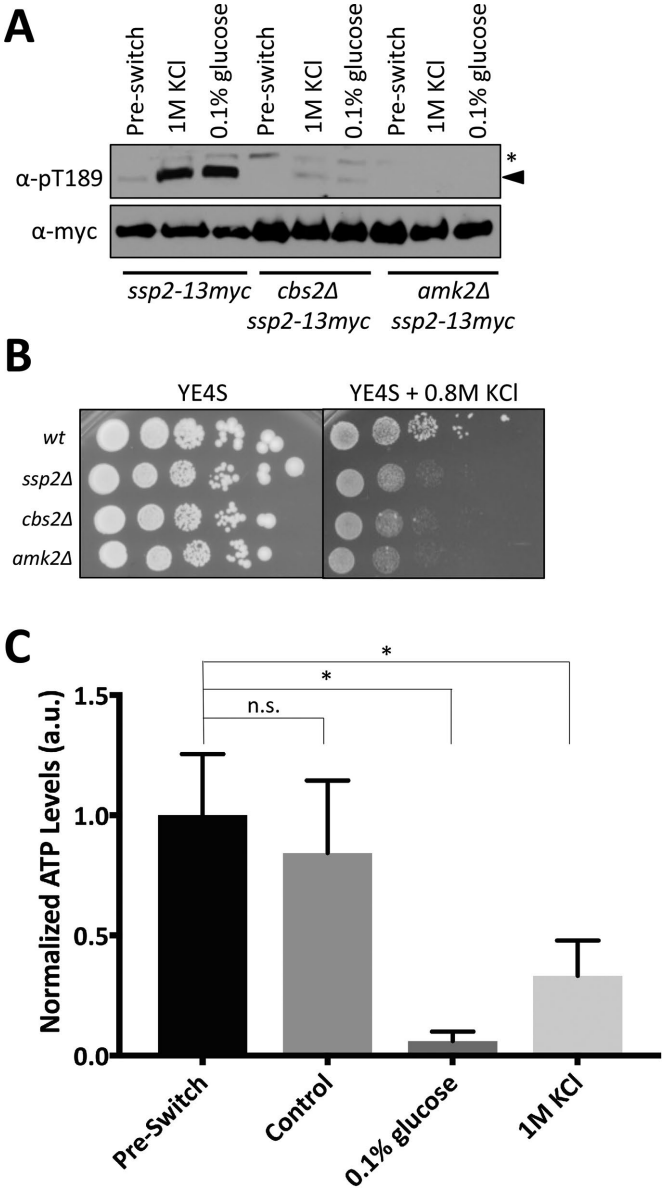

FIGURE 5: AMPK senses depletion of cellular ATP levels during osmotic stress. (A) Western blot showing activation of Ssp2-pT189 in wild-type, *cbs2*Δ, and *amk2*Δ cells in response to 1 M KCl. Preswitch (unstressed) and 0.1% glucose are used as a control for Ssp2 activation. Stress treatments were for 15 min. We used α-myc as a loading control for total Ssp2. For α-Ssp2-pT189, asterisks denote background bands, and arrowheads mark Ssp2-pT189 bands. (B) Tenfold serial dilutions of the indicated strains were spotted onto control (YE4S) plates or plates containing 0.8 M KCl. Cells were grown at 32°C. (C) Change in cellular ATP levels by 5-min treatment with the indicated stresses (preswitch and control were unstressed YE4S medium). ATP levels were measured and normalized as described in *Materials and Methods*. Mean ± SD. An unpaired *t* test was performed for statistical analyses, and *p* values were based on two-tailed distributions (**p* < 0.05).

to osmotic stress. These pathways include the osmolarity response and cell integrity pathways that activate SAP kinases Sty1 and Pmk1, respectively (Degols *et al.*, 1996, Toda *et al.*, 1996, Madrid *et al.*, 2006, 2007). We hypothesized that SAPK pathways might affect either the activation or the deactivation kinetics of AMPK. We tested this possibility by monitoring Ssp2-pT189 in *sty1*Δ and *pmk1*Δ cells. The timing of initial Ssp2-T189 phosphorylation was unaffected in these mutants, but Ssp2 activation persisted for a longer duration in cells lacking either of these SAPKs (Figures 7, A and B). The double mutant *sty1*Δ *pmk1*Δ did not show additive defects in the duration of Ssp2-pT189 (Figure 7C), suggesting the involvement of a shared downstream target. One common target between these SAPK pathways is the transcription factor Atf1 (Wilkinson *et al.*, 1996, Takada *et al.*, 2007). In *atf1*Δ cells, Ssp2-pT189 phosphorylation was present for a longer duration than in wild-type cells (Figure 7D) and was similar to that in *sty1*Δ and *pmk1*Δ mutants. This result suggests that Atf1-dependent transcription promotes inactivation of AMPK. The underlying mechanism could involve transcription of a specific factor that acts to promote Ssp2-T189 dephosphorylation. Alternatively, transcription could affect cellular processes that indirectly lead to AMPK inactivation as cells adapt to their new osmotic state. The extended duration of Ssp2-pT189 in *atf1*Δ cells was not as severe as in *sty1*Δ or *pmk1*Δ cells, suggesting that additional targets of the SAPK pathways are likely to contribute as well.

An important adaptive response for yeast cells under osmotic stress is the production of glycerol to restore turgor pressure (Aiba *et al.*, 1995; Minc *et al.*, 2009; Matsuzawa *et al.*, 2010). *S. pombe* does not have an active glycerol transport system (Lages *et al.*, 1999; Ferreira *et al.*, 2005; Minc *et al.*, 2009), and must generate glycerol de novo in two enzymatic steps: first, conversion of the glycolytic intermediate dihydroxyacetone phosphate (DHAP) to glycerol-3-phosphate (G3P) by Gpd1 and Gpd2 (Albertyn *et al.*, 1994, Eriksson *et al.*, 1995), and second, conversion of G3P to glycerol by glycerol-3-phosphatases Gpp1 and Gpp2 (Norbeck *et al.*, 1996). We hypothesized that Gpd1/2-dependent shifting of DHAP toward glycerol production may reduce ATP production, leading to AMPK activation. We tested a *gpd1*Δ *gpd2*Δ double mutant, which is predicted to prevent shuttling of glycolytic intermediates toward glycerol production and thereby might maintain high ATP levels. However, phosphorylation of Ssp2-T189 was not reduced in this mutant. Instead, Ssp2-pT189 levels persisted longer in the *gpd1*Δ *gpd2*Δ double mutant (Figure 8), suggesting that glycerol production through Gpd1/2 is not inhibiting ATP production during the osmotic stress response. Instead, glycerol production appears to contribute to AMPK inactivation during adaptation to osmotic stress.

DISCUSSION

We identified a dynamic regulatory system that transiently activates AMPK during osmotic stress in fission yeast cells. Our results provide a mechanistic model for both the initial activation step and the subsequent inactivation. When cells encounter osmotic stress, intracellular ATP levels drop, leading to increased phosphorylation levels of the activation loop of AMPK α subunit. This Ssp1-dependent activating modification appears within minutes and requires both the nucleotide-binding γ subunit and the scaffolding β subunit of AMPK. Thus AMPK activation during osmotic stress follows the canonical mechanism in which AMP-bound γ subunit generates a conformation that inhibits the rate of dephosphorylation of the α subunit by inactivating phosphatases (Davies *et al.*, 1995; Jiang and Carlson, 1996; Suter *et al.*, 2006, Sanders *et al.*, 2007, Rubenstein *et al.*, 2008, Mayer *et al.*, 2011). This suggests that the rate of Ssp2-T189 dephosphorylation represents the critical control point for the AMPK response during osmotic stress. A key and related implication of our results is that that osmotic stress induces energy stress in fission yeast cells.

Activation through this pathway is required for cells to resume growth in the new osmotic environment. At later time points, when cells have adapted to their new osmotic environment, AMPK is

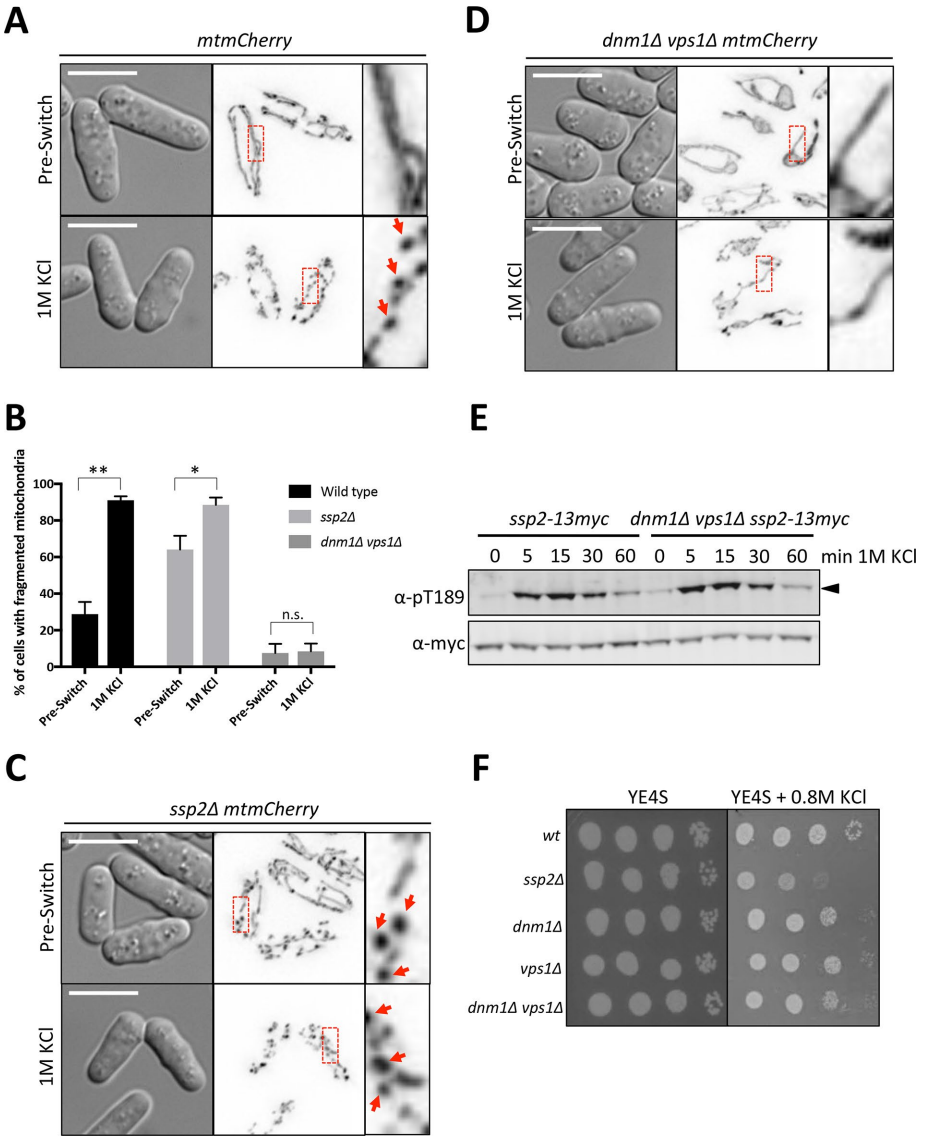

FIGURE 6: Fission of mitochondria during osmotic stress. (A) Representative images of mitochondria in wild-type cells before and after osmotic stress. (B) Quantification of cells expressing fragmented (beads-on-a-string) mitochondrial morphology, shown as a percentage of the total population. Three individual biological replicates were performed and >100 cells counted for each replicate. Mean ± SD. An unpaired *t* test was performed for statistical analysis with *p* values shown (*$p < 0.05$, **$p < 0.01$) as determined based on a two-tailed distribution. (C) Representative images of mitochondria in *ssp2*Δ cells before and after osmotic stress. (D) Representative images of mitochondria in *dnm1*Δ *vps1*Δ cells before and after osmotic stress. For A, C, and D, images on the left are DIC, and images in middle are corresponding inverted maximum projections for 0.2-µm-spaced *z*-sections through the entire cell (25 steps for 5 µm total). The red boxes are zoomed in on the right. Arrows denote "beaded" morphology. Scale bars, 5 µm. (E) Western blot showing activation kinetics of Ssp2-pT189 in *dnm1*Δ *vps1*Δ cells vs. wild-type cells in response to 1 M KCl osmotic stress. We used α-myc as a loading control for total Ssp2. (F) Tenfold serial dilutions of the indicated strains were spotted onto control (YE4S) plates or YE4S plates containing 0.8 M KCl. Cells were grown at 32°C.

inactivated. We found that SAPK pathways, which trigger transcriptional responses for osmotic adaptation, are required for efficient AMPK inactivation. This transient activation mechanism is distinct from the mechanism in budding yeast, in which sustained activation of AMPK is triggered by salt stress but not by general osmotic stress (Hong and Carlson, 2007; Ye *et al.*, 2008). The role of energy sensing in this budding yeast response has not been examined. It is interesting to note that AMPK is required for both budding yeast and fission yeast to survive in the conditions that activate AMPK. The different conditions that activate AMPK in one cell type versus another likely reflect differences in how the cell types couple energy homeostasis with the response to these conditions.

Our results raise a number of intriguing questions for future study. For example, what causes ATP levels to decrease during osmotic stress? This change could result from decreased production or from increased consumption of ATP. Following this logic, we tested the possibility that osmotic stress alters mitochondria, the major source of cellular ATP production. We observed dramatic fragmentation of mitochondria during osmotic stress, consistent with past work in budding yeast (Morris *et al.*, 1986). However, blocking mitochondrial fission with the *dnm1*Δ *vps1*Δ mutant had no effect on the kinetics of AMPK activation. Additional damage and/or changes to mitochondria beyond fragmentation may still contribute to regulation of intracellular ATP during osmotic stress. Note that increased transcription of mitochondrial enzymes, such as COX6, under hyperosmotic stress in budding yeast depends on AMPK and is essential for cell survival (Pastor *et al.*, 2009). This raises the possibility of bidirectional signaling between mitochondria and AMPK during the osmotic stress response.

It will also be interesting to compare the downstream effects of AMPK signaling during osmotic stress versus glucose depletion. Osmotic stress activates AMPK transiently, whereas glucose depletion leads to sustained AMPK activation. Further, the level of AMPK activation in both conditions depends on the degree of stress. Altering both the magnitude and the kinetics of activation can have dramatic effects on different downstream AMPK substrates. We observed regulation of the fission yeast AMPK target Scr1 during osmotic stress, and this regulation followed the timing of AMPK activation and inactivation. Scr1 is a transcription factor that negatively regulates expression of the glucose transporter Ght5 (Matsuzawa *et al.*, 2012, Saitoh *et al.*, 2015). Although normally in the nucleus, Scr1 is retained in the cytoplasm when phosphorylated by AMPK, leading to Ght5 expression. This connection to glucose transporter expression may relate to our findings because osmotic stress has been shown to stimulate both glucose transport and translocation of glucose transporters in mammalian cells (Forsayeth and Gould, 1981; Chen *et al.*, 1997). In these other systems, AMPK activation positively regulates glucose transport by increasing GLUT4 transcription, GLUT4 translocation to the plasma membrane, and stimulation of GLUT1 activity (Hayashi *et al.*, 1998,

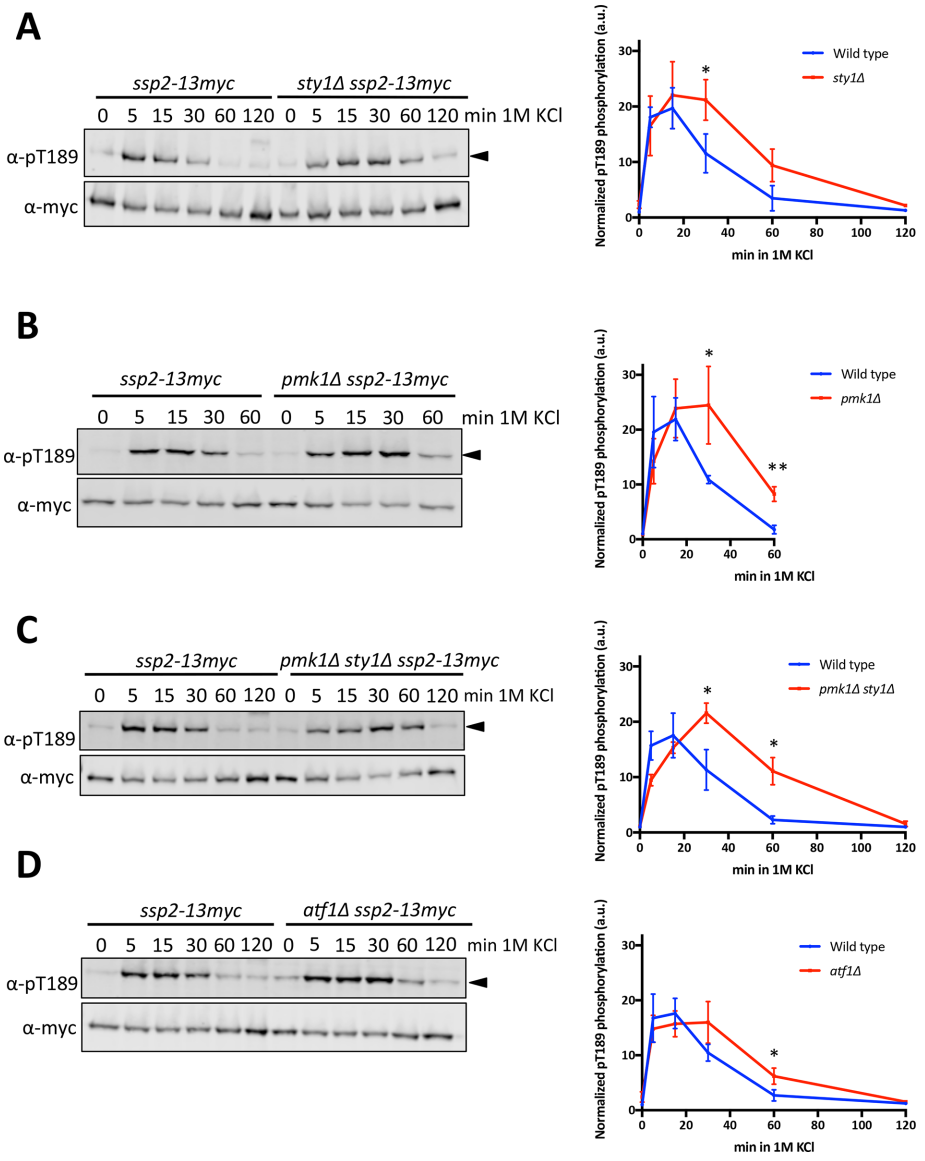

FIGURE 7: SAPK cascades contribute to deactivation of Ssp2. (A) Activation kinetics of Ssp2-pT189 in wild-type and *sty1*Δ cells in response to 1 M KCl osmotic stress. Left, Western blot. Right, quantification of three biological replicates. (B) Activation kinetics of Ssp2-pT189 in wild-type and *pmk1*Δ cells in response to 1 M KCl osmotic stress. Left, Western blot. Right, quantification of three biological replicates. (C) Activation kinetics of Ssp2-pT189 in wild-type and *pmk1*Δ *sty1*Δ cells in response to 1 M KCl osmotic stress. Left, Western blot. Right, quantification of three biological replicates. (D) Activation kinetics of Ssp2-pT189 in wild-type and *atf1*Δ cells in response to 1 M KCl osmotic stress. Left, Western blot. Right, quantification of three biological replicates. For all results, α-myc was used as a loading control for total Ssp2. Values displayed are the mean ± SD based on three biological replicates. An unpaired *t* test was performed for statistical analyses, and *p* values were based on two-tailed distributions (**p* < 0.05, ***p* < 0.01).

2000; Kurth-Kraczek *et al.*, 1999; Barnes *et al.*, 2002; McGee *et al.*, 2008; Lieburg-Apers *et al.*, 2016). Therefore AMPK activation may up-regulate glucose transport to counteract decreasing levels of ATP during osmotic stress. This possibility may be coordinated with other AMPK activities, such as increasing autophagy for adaptation to osmotic stress (Jiang *et al.*, 2015). This AMPK signaling during osmotic stress is likely to intersect with other SAPK pathways activated at the same time.

We identified at least one source of cross-talk between AMPK and SAPK pathways under osmotic stress. Deletion of Sty1, Pmk1, and their common target—the transcription factor Atf1—led to prolonged activation of AMPK under osmotic stress. A different form of cross-talk between AMPK and the SAPK Hog1 has been observed under low-glucose conditions in budding yeast, where starvation-independent activation of Snf1 was sufficient to activate Hog1 (Piao *et al.*, 2012). These combined findings raise the possibility of a delayed negative feedback loop by which AMPK activates SAPK, which contributes to AMPK inactivation through transcription factors such as Atf1. In addition, Gpd1 transcription is regulated by Sty1-Atf1 signaling, and Gpd1 may be an important target contributing to AMPK inactivation, supported by the increased duration of Ssp2-pT189 in *gpd1*Δ *gpd2*Δ mutants (Figure 8; Chen *et al.* 2003; Reiter *et al.* 2008). Such a mechanism could facilitate cellular adaptation during conditions such as osmotic stress. Because both the AMPK and SAPK signaling pathways are differentially activated by a range of environmental stresses, it will be interesting to test how their connection changes with growth conditions.

MATERIALS AND METHODS

Yeast strains and growth

Standard *S. pombe* media and methods were used (Moreno *et al.*, 1991). Strains used in this study are listed in Supplemental Table S1; plasmids are listed in Supplemental Table S2. Gene tagging and deletion were performed using PCR and homologous recombination (Bähler *et al.*, 1998), and integrations were verified by colony PCR, microscopy, and/or Western blot. The nonphosphorylatable *ssp2-T189A* and *cdr2-T166A* mutants were generated using QuikChange II mutagenesis (Stratagene) and integrated at the endogenous locus using 5-fluoroorotic acid counterselection (Deng *et al.*, 2017). To cross the mutant *ssp1*Δ, a pJK148 plasmid with *6His2HA-ssp1+* was integrated at the *leu1+* locus of JM1220 (*ssp1*Δ*::kanR leu1-32* h+), and *leu1-32 kanR* progeny were selected from subsequent crosses. To cross the mutant *sty1*Δ, JM1168 (*sty1*Δ*::natR ura4-D18 leu1-32 ade6-M21X h+* [pREP4X-sty1+::ura4+]) was provided by Francisco Navarro (The Rockefeller University). The strain expressing mCherry targeted to the mitochondrial matrix (*mtmCherry*) was provided by Johan Paulsson (Harvard Medical School; Jajoo *et al.*, 2016). For the growth assays in Figures 3D, 5B, and 6F, cells were spotted by 10-fold serial dilution onto either YE4S (yeast extract with four supplements) plus 3% glucose or YE4S plus 3% glucose plus 0.8 M KCl plates and incubated at 32°C.

Western blots and quantification

For Western blots, logarithmic-phase cells at OD_{595} = 2 were rapidly harvested and snap-frozen from unstressed growth or indicated treatment. Whole-cell extracts were prepared by resuspending cells

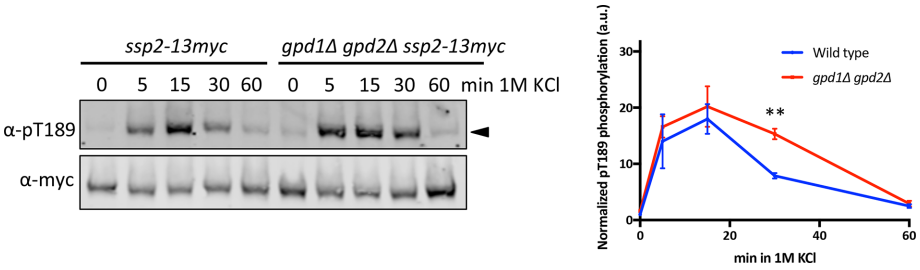

FIGURE 8: Glycerol biosynthesis contributes to deactivation of Ssp2. Western blot and quantification showing activation kinetics of Ssp2-pT189 in wild-type and *gpd1Δ gpd2Δ* cells in response to 1 M KCl osmotic stress. We used α-myc as loading control for total Ssp2. Values displayed are the mean ± SD based on three individual biological replicates. An unpaired *t* test was performed for statistical analyses, and *p* values were based on two-tailed distributions (**$p < 0.01$).

in sample buffer (65 mM Tris, pH 6.8, 3% SDS, 10% glycerol, 10% 2-mercaptoethanol, 50 mM NaF, 50 mM β-glycerophosphate, 1 mM sodium orthovanadate, and protease inhibitor cocktail) and lysing with acid-washed glass beads (Sigma-Aldrich) in a Mini-beadbeater-16 (BioSpec, Bartlesville, OK; two cycles of 2 min at maximum speed in a cold room). Lysates were briefly centrifuged to pellet insoluble material, and supernatant was isolated as whole-cell extract. All samples shown are whole-cell extracts unless otherwise indicated. Western blots were probed with anti-myc (SC-40; Santa Cruz Biotechnology), anti-Ssp2-pT189, and anti-Cdr2-pT166. Rabbit anti-Ssp2-pT189 antibody was generated against the phosphopeptide GNFLK[pT]SCGSPNY (21st Century Biochemicals; Deng *et al.*, 2017). Rabbit anti–Cdr2-pT166 antibody was generated against the phosphopeptide GKLLQ[pT]SCGSPHY (21st Century Biochemicals; Deng *et al.*, 2014). For Figures 1D, 2B, 3B, 6E, 7, A–D, and 8, Western blots were probed with goat anti-rabbit and goat anti-mouse secondary antibodies (LI-COR) and developed on an Odyssey CLx Imaging System (LI-COR) and quantified using Image Studio Lite (LI-COR). To quantify normalized pT189 phosphorylation, a rectangle was drawn around each band, and intensity of the bands was measured after background subtraction for both pT189 and myc. Ratio of Ssp2-pT189 (pT189 signal) to total Ssp2 (myc signal) was calculated. Ssp2-pT189/Total Ssp2 ratios for each time point were normalized to wild-type preswitch levels to show relative changes in phosphorylation. The same method was used to quantify normalized pT166 phosphorylation for Cdr2-pT166 in Figure 3, B and C. For quantification, three individual biological replicates were performed, and the mean ± SD is displayed. For statistical analyses, unpaired *t* tests assuming unequal variances were performed, and *p* values were determined by two-tailed distribution (*$p < 0.05$ and **$p < 0.01$). For all statistical analyses, StatPlus:Mac (Analyst Soft) was used.

Determination of ATP levels

For Figure 5C, logarithmic-phase cells at $OD_{595} = 2$ were collected during unstressed growth in YE4S (Pre-Switch) or in stressed growth after resuspension in YE4S containing 1 M KCl or 0.1% glucose. As a control, cells were resuspended in unstressed YE4S (Control). Cell pellets were resuspended in 200 µl ATP assay buffer (50 mM 4-(2-hydroxyethyl)-1-piperazineethanesulfonic acid, pH 8.0, 100 mM KCl, 1 mM EDTA, 1 mM dithiothreitol, and 1 mM phenylmethylsulfonyl fluoride) with 400 µl of acid-washed glass beads (Sigma-Aldrich) and then lysed in a Mini-beadbeater-16 (two cycles of 2 min at maximum speed). Cell extracts were pelleted by centrifugation at 4°C into a fresh Eppendorf tube. Next 1:1 volumes of cell extract:luciferase reagent (ATP Bioluminescence Assay Kit; Sigma-Aldrich) were mixed in a ThermoFisher Nunc white, flat, 96-well cell culture plate, and luminescence was instantly measured using a Tecan Infinite M1000 Pro microplate reader. ATP concentrations for each sample were calculated from an ATP standard curve (Sigma-Aldrich). Average ATP concentrations were normalized to protein concentrations, which were measured using a DC protein assay kit (Bio-Rad) with standard curve obtained from bovine serum albumin. ATP levels were normalized to Pre-Switch. For each biological replicate, three technical replicates were performed and then averaged. Three individual biological replicates were performed to generate the displayed mean ± SD. For statistical analyses, unpaired *t* tests assuming unequal variances were performed, and *p* values were determined by two-tailed distribution (*$p < 0.05$ and **$p < 0.01$). For all statistical analyses, StatPlus:Mac (Analyst Soft) was used.

Microscopy

Images were obtained at room temperature using a DeltaVision Imaging System (Applied Precision/GE Healthcare) with a customized Olympus IX-71 inverted wide-field microscope, a Photometrics CoolSNAP HQ2 camera, and Insight solid-state illumination unit. Images obtained as a series of *z*-stacks were processed by iterative deconvolution in SoftWoRx Software (Applied Precision/GE Healthcare). All further image analysis was performed on ImageJ (National Institutes of Health). Unless otherwise indicated, a single focal plane from the cell middle was imaged in liquid medium under a coverslip. For Figures 1E and 4A, cells were imaged using a CellASIC ONIX Y04C Microfluidics Plate in conjunction with the ONIX microfluidic perfusion platform (CellASIC). Before loading of cells, the imaging chambers were prewashed with fresh EMM4S medium (Figure 1E) or YE4S medium (Figure 4A). Cells were loaded for 5–15 s at 8 psi. Before imaging, cells were acclimated in the imaging chamber for at least 1 h with fresh unstressed medium flowing at 1 psi. As a control for any influence from changing the input source, medium switches from unstressed medium to unstressed medium (in different input wells) were used. For osmotic stress, medium switches from unstressed medium to medium containing 1 M KCl were used. For Figure 1F, >50 cells were counted to determine the percentage of cells with Scr1 nuclear localization for three independent biological replicates. For Figure 4B, only cells present in the imaging chamber for the entire duration were counted. Cells flowing in or out of the imaging chamber were not included in the quantification. For images in Figure 6 A, C, and D, maximum intensity projections were generated using 0.2-µm focal planes throughout the entire cell (25 steps, 5 µm total). Cells were grown in unstressed medium, and the culture was split in half: one half of the cells were imaged unstressed (Pre-Switch), and the other half was resuspended in 1 M KCl for 10 min before imaging ("1 M KCl"). For quantification in Figure 6B, cells containing "tubular" mitochondria were considered unfragmented (zoomed region in Figure 6A, Pre-Switch). Cells without tubular mitochondria that appeared as beaded were considered fragmented (zoomed region on Figure 6A; "1 M KCl" and red arrows). For quantification, three individual biological replicates were performed, and the mean ± SD is displayed. For statistical analyses, unpaired *t* tests assuming unequal variances were performed, and *p* values were determined by two-tailed distribution (*$p < 0.05$ and **$p < 0.01$). For all statistical analyses, StatPlus:Mac (Analyst Soft) was used.

ACKNOWLEDGMENTS

We thank members of the Moseley lab for comments on the manuscript, as well as Ambrose Cheung and Charles Barlowe at Dartmouth for sharing equipment. We also thank Kathy Gould, Nic Jones, Francisco Navarro, Paul Nurse, Pilar Pérez, and Johan Paulsson for sharing strains. This work was supported by grants from the American Cancer Society (RSG-15-140-01-CCG) and the National Institutes of Health (R01 GM099774) to J.B.M.

REFERENCES

Aiba H, Yamada H, Ohmiya R, Mizuno T (1995). The osmo-inducible gpd1+ gene is a target of the signaling pathway involving Wis1 MAP-kinase kinase in fission yeast. FEBS Lett 376, 199–201.

Albertyn J, Hohmann S, Thevelein JM, Prior BA (1994). GPD1, which encodes glycerol-3-phosphate dehydrogenase, is essential for growth under osmotic stress in Saccharomyces cerevisiae, and its expression is regulated by the high-osmolarity glycerol response pathway. Mol Cell Biol 14, 4135–4144.

Bähler J, Wu JQ, Longtine MS, Shah NG, McKenzie A, Steever AB, Wach A, Philippsen P, Pringle JR (1998). Heterologous modules for efficient and versatile PCR-based gene targeting in Schizosaccharomyces pombe. Yeast 14, 943–951.

Barnes K, Ingram JC, Porras OH, Barros LF, Hudson ER, Fryer LGD, Foufelle F, Carling D, Hardie DG, Baldwin SA (2002). Activation of GLUT1 by metabolic and osmotic stress: potential involvement of AMP-activated protein kinase (AMPK). J Cell Sci 115, 2433–2442.

Celenza JL, Carlson M (1986). A yeast gene that is essential for release from glucose repression encodes a protein kinase. Science 233, 1175–1180.

Chen D, Elmendorf JS, Olson AL, Li X, Earp HS, Pessin JE (1997). Osmotic shock stimulates GLUT4 translocation in 3T3L1 adipocytes by a novel tyrosine kinase pathway. J Biol Chem 272, 27401–27410.

Chen D, Toone WM, Mata J, Lyne R, Burns G, Kivinen K, Brazma A, Jones N, Bähler J (2003). Global transcriptional responses of fission yeast to environmental stress. Mol Biol Cell 14, 214–229.

Corton JM, Gillespie JG, Hardie DG (1994). Role of the AMP-activated protein kinase in the cellular stress response. Curr Biol 4, 315–324.

Davie E, Forte GMA, Petersen J (2015). Nitrogen regulates AMPK to control TORC1 signaling. Curr Biol 25, 445–454.

Davies SP, Helps NR, Cohen PT, Hardie DG (1995). 5′-AMP inhibits dephosphorylation, as well as promoting phosphorylation, of the AMP-activated protein kinase. Studies using bacterially expressed human protein phosphatase-2C alpha and native bovine protein phosphatase-2AC. FEBS Lett 377, 421–425.

Degols G, Shiozaki K, Russell P (1996). Activation and regulation of the Spc1 stress-activated protein kinase in Schizosaccharomyces pombe. Mol Cell Biol 16, 2870–2877.

Deng L, Baldissard S, Kettenbach AN, Gerber SA, Moseley JB (2014). Dueling kinases regulate cell size at division through the SAD kinase Cdr2. Curr Biol 24, 428–433.

Deng L, Lee ME, Schutt K, Moseley JB (2017). Phosphatases generate signal specificity downstream of Ssp1 kinase in fission yeast. Mol Cell Biol 37, e00494-16.

DeVit MJ, Waddle JA, Johnston M (1997). Regulated nuclear translocation of the Mig1 glucose repressor. Mol Biol Cell 8, 1603–1618.

Elbing K, Rubenstein EM, McCartney RR, Schmidt MC (2006). Subunits of the Snf1 kinase heterotrimer show interdependence for association and activity. J Biol Chem 281, 26170–26180.

Emerling BM, Weinberg F, Snyder C, Burgess Z, Mutlu GM, Viollet B, Budinger GR, Chandel NS (2009). Hypoxic activation of AMPK is dependent on mitochondrial ROS but independent of an increase in AMP/ATP ratio. Free Radic Biol Med 46, 1386–1391.

Eriksson P, André L, Ansell R, Blomberg A, Adler L (1995). Cloning and characterization of GPD2, a second gene encoding sn-glycerol 3-phosphate dehydrogenase (NAD+) in Saccharomyces cerevisiae, and its comparison with GPD1. Mol Microbiol 17, 95–107.

Evans AM, Mustard KJW, Wyatt CN, Peers C, Dipp M, Kumar P, Kinnear NP, Hardie DG (2005). Does AMP-activated protein kinase couple inhibition of mitochondrial oxidative phosphorylation by hypoxia to calcium signaling in O2-sensing cells? J Biol Chem 280, 41504–41511.

Ferreira C, van Voorst F, Martins A, Neves L, Oliveira R, Kielland-Brandt MC, Lucas C, Brandt A (2005). A member of the sugar transporter family, Stl1p Is the Glycerol/H+ symporter in Saccharomyces cerevisiae. Mol Biol Cell 16, 2068–2076.

Forsayeth J, Gould MK (1981). Effects of hyperosmolarity on basal and insulin-stimulated muscle sugar transport. Am J Physiol 240, E263–E267.

Freitag SI, Wong J, Young PG (2014). Genetic and physical interaction of Ssp1 CaMKK and Rad24 14-3-3 during low pH and osmotic stress in fission yeast. Open Biol 4, 130127.

Fryer LG, Parbu-Patel A, Carling D (2002). The anti-diabetic drugs rosiglitazone and metformin stimulate AMP-activated protein kinase through distinct signaling pathways. J Biol Chem 277, 25226–25232.

Hanyu Y, Imai KK, Kawasaki Y, Nakamura T, Nakaseko Y, Nagao K, Kokubu A, Ebe M, Fujisawa A, Hayashi T, *et al*. (2009). *Schizosaccharomyces pombe* cell division cycle under limited glucose requires Ssp1 kinase, the putative CaMKK, and Sds23, a PP2A-related phosphatase inhibitor. Genes Cells 14, 539–554.

Hawley SA, Boudeau J, Reid JL, Mustard KJ, Udd L, Mäkelä TP, Alessi DR, Hardie DG (2003). Complexes between the LKB1 tumor suppressor, STRAD alpha/beta and MO25 alpha/beta are upstream kinases in the AMP-activated protein kinase cascade. J Biol 2, 28.

Hawley SA, Ross FA, Chevtzoff C, Green KA, Evans A, Fogarty S, Towler MC, Brown LJ, Ogunbayo OA, Evans AM, Hardie DG (2010). Use of cells expressing γ subunit variants to identify diverse mechanisms of AMPK activation. Cell Metab 11, 554–565.

Hayashi T, Hirshman MF, Fujii N, Habinowski SA, Witters LA, Goodyear LJ (2000). Metabolic stress and altered glucose transport: activation of AMP-activated protein kinase as a unifying coupling mechanism. Diabetes 49, 527–531.

Hayashi T, Hirshman MF, Kurth EJ, Winder WW, Goodyear LJ (1998). Evidence for 5′ AMP-activated protein kinase mediation of the effect of muscle contraction on glucose transport. Diabetes 47, 1369–1373.

Hong S-P, Carlson M (2007). Regulation of snf1 protein kinase in response to environmental stress. J Biol Chem 282, 16838–16845.

Hong S-P, Leiper FC, Woods A, Carling D, Carlson M (2003). Activation of yeast Snf1 and mammalian AMP-activated protein kinase by upstream kinases. Proc Nat Acad Sci USA 100, 8839–8843.

Iseli TJ, Walter M, van Denderen BJW, Katsis F, Witters LA, Kemp BE, Michell BJ, Stapleton D (2005). AMP-activated protein kinase beta subunit tethers alpha and gamma subunits via its C-terminal sequence (186-270). J Biol Chem 280, 13395–13400.

Jajoo R, Jung Y, Huh D, Viana MP, Rafelski SM, Springer M, Paulsson J (2016). Accurate concentration control of mitochondria and nucleoids. Science 351, 169–172.

Jiang L-B, Cao L, Yin X-F, Yasen M, Yishake M, Dong J, Li X-L (2015). Activation of autophagy via Ca(2+)-dependent AMPK/mTOR pathway in rat notochordal cells is a cellular adaptation under hyperosmotic stress. Cell Cycle 14, 867–879.

Jiang R, Carlson M (1996). Glucose regulates protein interactions within the yeast SNF1 protein kinase complex. Genes Dev 10, 3105–3115.

Jourdain I, Sontam D, Johnson C, Dillies C, Hyams JS (2008). Dynamin-dependent biogenesis, cell cycle regulation and mitochondrial association of peroxisomes in fission yeast. Traffic 9, 353–365.

Kurth-Kraczek EJ, Hirshman MF, Goodyear LJ, Winder WW (1999). 5′ AMP-activated protein kinase activation causes GLUT4 translocation in skeletal muscle. Diabetes 48, 1667–1671.

Lages F, Silva-Graca M, Lucas C (1999). Active glycerol uptake is a mechanism underlying halotolerance in yeasts: a study of 42 species. Microbiology 145, 2577–2585.

Lieburg-Apers DC, Wagenaars JAL, Smeitink JAM, Willems PHGM, Koopman WJH (2016). Acute stimulation of glucose influx upon mitoenergetic dysfunction requires LKB1, AMPK, Sirt2 and mTOR-RAPTOR. J Cell Sci 129, 4411–4423.

Lizcano JM, Göransson O, Toth R, Deak M, Morrice NA, Boudeau J, Hawley SA, Udd L, Mäkelä TP, Hardie DG, Alessi DR (2004). LKB1 is a master kinase that activates 13 kinases of the AMPK subfamily, including MARK/PAR-1. EMBO J 23, 833–843.

Luo L, Jiang S, Huang D, Lu N, Luo Z (2015). MLK3 phophorylates AMPK independently of LKB1. PLoS One 10, e0123927.

Madrid M, Núñez A, Soto T, Vicente-Soler J, Gacto M, Cansado J (2007). Stress-activated protein kinase-mediated down-regulation of the cell integrity pathway mitogen-activated protein kinase Pmk1p by protein phosphatases. Mol Biol Cell 18, 4405–4419.

Madrid M, Soto T, Khong HK, Franco A, Vicente J, Pérez P, Gacto M, Cansado J (2006). Stress-induced response, localization, and regulation of the Pmk1 cell integrity pathway in Schizosaccharomyces pombe. J Biol Chem 281, 2033–2043.

Matsuzawa T, Fujita Y, Tohda H, Takegawa K (2012). Snf1-Like protein kinase Ssp2 regulates glucose derepression in schizosaccharomyces pombe. Eukaryotic Cell 11, 159–167.

Matsuzawa T, Ohashi T, Hosomi A, Tanaka N, Tohda H, Takegawa K (2010). The gld1 + gene encoding glycerol dehydrogenase is required for glycerol metabolism in Schizosaccharomyces pombe. Appl Microbiol Biotechnol 87, 715–727.

Mayer FV, Heath R, Underwood E, Sanders MJ, Carmena D, McCartney RR, Leiper FC, Xiao B, Jing C, Walker PA, *et al*. (2011). ADP regulates SNF1, the Saccharomyces cerevisiae homolog of AMP-activated protein kinase. Cell Metab 14, 707–714.

McGee SL, van Denderen BJW, Howlett KF, Mollica J, Schertzer JD, Kemp BE, Hargreaves M (2008). AMP-activated protein kinase regulates GLUT4 transcription by phosphorylating histone deacetylase 5. Diabetes 57, 860–867.

Minc N, Boudaoud A, Chang F (2009). Mechanical forces of fission yeast growth. Curr Biol 19, 1096–1101.

Moreno S, Klar A, Nurse P (1991). Molecular genetic analysis of fission yeast Schizosaccharomyces pombe. Methods Enzymol 194, 795–823.

Morris GJ, Winters L, Coulson GE, Clarke KJ (1986). Effect of osmotic stress on the ultrastructure and viability of the yeast saccharomyces cerevisiae. Microbiology 132, 2023–2034.

Nath N, McCartney RR, Schmidt MC (2003). Yeast Pak1 kinase associates with and activates Snf1. Mol Cell Biol 23, 3909–3917.

Norbeck J, Pahlman A-K, Akhtar N, Blomberg A, Adler L (1996). Purification and characterization of two isoenzymes of DL-glycerol-3-phosphatase from Saccharomyces cerevisiae. Identification of the corresponding GPP1 and GPP2 genes and evidence for osmotic regulation of Gpp2p expression by the osmosensing mitogen-activated protein kinase signal transduction pathway. J Biol Chem 271, 13875–13881.

Pastor MM, Proft M, Pascual-Ahuir A (2009). Mitochondrial function is an inducible determinant of osmotic stress adaptation in yeast. J Biol Chem 284, 30307–30317.

Piao H, MacLean Freed J, Mayinger P (2012). Metabolic activation of the HOG MAP kinase pathway by Snf1/AMPK regulates lipid signaling at the golgi: metabolic regulation golgi PI(4)P. Traffic 13, 1522–1531.

Reiter W, Watt S, Dawson K, Lawrence CL, Bähler J, Jones N, Wilkinson CRM (2008). Fission yeast MAP kinase Sty1 is recruited to stress-induced genes. J Biol Chem 283, 9945–9956.

Rubenstein EM, McCartney RR, Zhang C, Shokat KM, Shirra MK, Arndt KM, Schmidt MC (2008). Access denied: Snf1 activation loop phosphorylation is controlled by availability of the phosphorylated threonine 210 to the PP1 phosphatase. J Biol Chem 283, 222–230.

Rupeš I, Jia Z, Young PG (1999). Ssp1 promotes actin depolymerization and is involved in stress response and new end take-off control in fission yeast. Mol Biol Cell 10, 1495–1510.

Saitoh S, Mori A, Uehara L, Masuda F, Soejima S, Yanagida M (2015). Mechanisms of expression and translocation of major fission yeast glucose transporters regulated by CaMKK/phosphatases, nuclear shuttling, and TOR. Mol Biol Cell 26, 373–386.

Sanders MJ, Grondin PO, Hegarty BD, Snowden MA, Carling D (2007). Investigating the mechanism for AMP activation of the AMP-activated protein kinase cascade. Biochem J 403, 139–148.

Schmidt MC, McCartney RR (2000). beta-Subunits of Snf1 kinase are required for kinase function and substrate definition. EMBO J 19, 4936–4943.

Scott JW, Hawley SA, Green KA, Anis M, Stewart G, Scullion GA, Norman DG, Hardie DG (2004). CBS domains form energy-sensing modules whose binding of adenosine ligands is disrupted by disease mutations. J Clin Invest 113, 274–284.

Shackelford DB, Shaw RJ (2009). The LKB1-AMPK pathway: metabolism and growth control in tumour suppression. Nat Rev Cancer 9, 563–575.

Suter M, Riek U, Tuerk R, Schlattner U, Wallimann T, Neumann D (2006). Dissecting the role of 5′-AMP for allosteric stimulation, activation, and deactivation of AMP-activated protein kinase. J Biol Chem 281, 32207–32216.

Sutherland CM, Hawley SA, McCartney RR, Leech A, Stark MJR, Schmidt MC, Hardie DG (2003). Elm1p Is one of three upstream kinases for the saccharomyces cerevisiae SNF1 complex. Curr Biol 13, 1299–1305.

Takada H, Nishimura M, Asayama Y, Mannse Y, Ishiwata S, Kita A, Doi A, Nishida A, Kai N, Moriuchi S, *et al*. (2007). Atf1 is a target of the mitogen-activated protein kinase Pmk1 and regulates cell integrity in fission yeast. Mol Biol Cell 18, 4794–4802.

Toda T, Dhut S, Superti-Furga G, Gotoh Y, Nishida E, Sugiura R, Kuno T (1996). The fission yeast pmk1+ gene encodes a novel mitogen-activated protein kinase homolog which regulates cell integrity and functions coordinately with the protein kinase C pathway. Mol Cell Biol 16, 6752–6764.

Toyama EQ, Herzig S, Courchet J, Lewis TL, Losón OC, Hellberg K, Young NP, Chen H, Polleux F, Chan DC, Shaw RJ (2016). Metabolism. AMP-activated protein kinase mediates mitochondrial fission in response to energy stress. Science 351, 275–281.

Treitel MA, Kuchin S, Carlson M (1998). Snf1 protein kinase regulates phosphorylation of the Mig1 repressor in Saccharomyces cerevisiae. Mol Cell Biol 18, 6273–6280.

Valbuena N, Moreno S (2012). AMPK phosphorylation by Ssp1 is required for proper sexual differentiation in fission yeast. J Cell Sci 125, 2655–2664.

Wilkinson MG, Samuels M, Takeda T, Toone WM, Shieh JC, Toda T, Millar JB, Jones N (1996). The Atf1 transcription factor is a target for the Sty1 stress-activated MAP kinase pathway in fission yeast. Genes Dev 10, 2289–2301.

Wilson WA, Hawley SA, Hardie DG (1996). Glucose repression/derepression in budding yeast: SNF1 protein kinase is activated by phosphorylation under derepressing conditions, and this correlates with a high AMP:ATP ratio. Curr Biol 6, 1426–1434.

Woods A, Johnstone SR, Dickerson K, Leiper FC, Fryer LGD, Neumann D, Schlattner U, Wallimann T, Carlson M, Carling D (2003). LKB1 is the upstream kinase in the AMP-activated protein kinase cascade. Curr Biol 13, 2004–2008.

Ye T, Elbing K, Hohmann S (2008). The pathway by which the yeast protein kinase Snf1p controls acquisition of sodium tolerance is different from that mediating glucose regulation. Microbiology 154, 2814–2826.